Tissue hypoxia and alterations in microvascular architecture predict glioblastoma recurrence in humans

Andreas Stadlbauer[1,2], Thomas M. Kinfe[1,3], Ilker Eyüpoglu[1], Max Zimmermann[1,4], Melitta Kitzwögerer[5], Klaus Podar[6], Michael Buchfelder[1], Gertraud Heinz[2], Stefan Oberndorfer[7,*], Franz Marhold[8,*]

[1]Department of Neurosurgery, Friedrich-Alexander University (FAU) Erlangen-Nürnberg, Erlangen, Germany

[2]Institute of Medical Radiology, University Clinic St. Pölten, Karl Landsteiner University of Health Sciences, St. Pölten, Austria

[3]Division of Functional Neurosurgery and Stereotaxy, Friedrich-Alexander University (FAU) Erlangen-Nürnberg, Erlangen, Germany

[4]Department of Preclinical Imaging and Radiopharmacy, University of Tübingen, Tübingen, Germany

[5]Department of Pathology, University Clinic of St. Pölten, St. Pölten, Austria

[6]Department of Internal Medicine 2, University Hospital Krems, Karl Landsteiner University of Health Sciences, Krems, Austria

[7]Department of Neurology, University Clinic of St. Pölten, Karl Landsteiner University of Health Sciences, St. Pölten, Austria

[8]Department of Neurosurgery, University Clinic of St. Pölten, Karl Landsteiner University of Health Sciences, St. Pölten, Austria

*These authors have contributed equally to this study as senior author.

Running title. Physiological MRI of glioblastoma recurrence

Corresponding Author: Prof. Dr. Andreas Stadlbauer, Department of Neurosurgery, University of Erlangen-Nürnberg, Schwabachanlage 6, 91054 Erlangen, Germany, Phone: +49-9131-8534259, Fax: +49-9131-8534271, email: andi@nmr.at

Conflict of Interest. The authors declared no potential conflicts of interest with respect to the research, authorship, and/or publication of this article

Word Count. 4931

Number of figures / tables. 4 / 0

Translational Relevance

Currently, conventional MRI-based concepts for the accurate and early stage diagnosis and therapy of recurrent glioblastoma are sparse. This lead to a delayed detection and therapy with consecutively decreased overall survival of patients with recurrent glioblastoma. While other neuroimaging modalities like PET have been applied to detect early recurrence of glioblastoma, tailored MRI-based diagnosis and therapy deserves further attention. Given these facts and in order to close this open gap, we herein present a physiological MRI protocol with the capability to determine microvascular architecture and perfusion, neovascularization activity, oxygen metabolism, and hypoxia relevant for the early detection of glioblastoma recurrence and suitable to be implemented into clinical neuro-oncological practice. We found decreasing microvascular density and perfusion, which was associated with intensifying hypoxia and an up-regulated neovascularization 27 weeks prior to radiological recurrence detection with conventional MRI. The authors believe that these findings are of relevance and deserve further enhanced attention.

ABSTRACT

Purpose: Insufficient control of infiltrative glioblastoma cells is a major cause of treatment failure and tumor recurrence. Hence, detailed insights into pathophysiological changes that precede glioblastoma recurrence are needed in order to develop more precise neuroimaging modalities for tailored diagnostic monitoring and therapeutic approaches.

Experimental Design: Overall 168 physiological magnetic resonance imaging (MRI) follow-up examinations of 56 glioblastoma patients who developed recurrence after standard therapy were retrospectively evaluated, i.e. two post-standard-therapeutic follow-ups before and one at radiological recurrence. MRI biomarkers for microvascular architecture and perfusion, neovascularization activity, oxygen metabolism, and hypoxia were determined for brain areas that developed in the further course into recurrence and for the recurrent glioblastoma itself. The temporal pattern of biomarker changes were fitted with locally-estimated-scatterplot-smoothing (LOESS) functions and analyzed for pathophysiological changes preceding radiological glioblastoma recurrence.

Results: Our MRI approach demonstrated early pathophysiological changes prior to radiological glioblastoma recurrence in all patients. Analysis of the time courses revealed a model for the pathophysiology of glioblastoma recurrence: 190 days prior to radiological recurrence, vascular cooption by glioblastoma cells induced vessel regression detected as decreasing vessel density/perfusion and increasing hypoxia. 70 days later, neovascularization activity was upregulated which re-increased vessel density and perfusion. Hypoxia, however, continued to intensify for 30 days and peaked 90 days before radiological recurrence.

Conclusions: Hypoxia may represent an early sign for GBM recurrence. This might become useful in the development of new combined diagnostic-therapeutic approaches for tailored clinical management of recurrent glioblastoma. Further preclinical and in-human studies are required for validation and evaluation.

Introduction

Glioblastoma (GBM) represents the most frequent and malign primary brain tumor in adults that is characterized by a tumor bulk with rapid cellular proliferation and active neovascularization surrounded by the tumor border zone with diffuse infiltration into the adjacent brain tissue. This aggressive and invasive behavior of GBM cells limits complete surgical resection and challenges adjuvant therapies by irradiation means. Inadequate control of these infiltrative GBM cells is a major cause of treatment failure and tumor relapse which occurs inevitable typically 6 – 7 months after initial diagnosis (1) in close proximity (1 – 2 cm) to the primary tumor bulk in the initial infiltration zone (2). Remarkably, fundamental knowledge of the (spatial-temporal) pathophysiology of GBM recurrence development is slowly emerging (3), however, new concept for early and reliable detection of recurrent GBM are urgently needed.

GBM cells infiltrate the surrounding neural tissue through two principal pathways, namely the perivascular space or the brain parenchyma, especially along white matter tracts (4). The extracellular spaces in the parenchyma, however, are narrow and more tortuous than the perivascular space. Experiments in animal models have shown that the vast majority (>85%) of GBM cells migrate along pre-existing blood vessels (5,6), a process known as vascular cooption (7), and disrupt the astrocyte-vasculature interaction (8). Subsequently, tumor cells organize themselves into cuffs around microvessels accompanied by upregulation of angiopoietin-2 (ANG-2) in the coopted vessels (7). This is associated with vascular regression leading to a decrease in tissue oxygen tension (hypoxia), hypoxia induced vascular endothelial growth factor (VEGF) expression (9), and eventually to the development of new vessels, a process known as neovascularization (9). Thereby, this infiltrative tumor niche either becomes part of the expanding tumor bulk or develops into a new tumor mass (10).

These biological processes of GBM progression are most likely relevant for the development of recurrences and combined assessment of microvascular architecture, oxygen metabolism, and neovascularization activity might elucidate pathophysiological mechanisms involved in therapy resistance and tumor recurrence. Given these facts, these parameters might represent clinically relevant novel imaging biomarkers for the early detection of GBM recurrence. Most of the available neuroimaging techniques, however, do not allow a combined investigation of these different processes requiring multiple examinations with different modalities which in turn are not well suited for in-vivo investigations in humans due to their invasiveness (oxygen electrodes or biopsies), or their limited availability and high costs (positron emission tomography, PET). This hinders the implementation of such outcome measures for clinical routine use. In order to counterbalance these limitations, we previously presented a novel multiparametric magnetic resonance imaging (MRI) approach scoping to obtain quantitative information about microvascular architecture and perfusion, neovascularization activity, and oxygen metabolism in glioma patients (11–14).

In this study, we hypothesized that our MRI approach offers the capability to detect pathophysiological changes in the early developmental stage of GBM recurrence in humans. Hence, the aims of our study were (**i**) to investigate the pathophysiological changes preceding GBM recurrence; (**ii**) to assess the interdependence of the physiological parameters prior to radiological recurrence; and (**iii**) to determine of pathophysiological differences in the development of locally and distantly recurrent GBM.

Materials and Methods

Patients

The institutional review board approved this retrospective study. Written informed consent in accordance with the ethical standards of the Helsinki Declaration of 1975 and its later amendments was obtained from all enrolled patients. A prospectively populated institutional database was searched for patients with glioblastoma (World Health Organization, WHO grade IV) who were treated according to standard of care, i.e. maximal safe and radical resection, radiotherapy, and concomitant and adjuvant chemotherapy with temozolomide (15), and received MR examinations with our MRI study protocol between July 2015 and April 2020. Inclusion criteria were as follows: (**i**) aged ≥ 18 years; (**ii**) pathologically confirmed GBM based on the WHO histological grading system; (**iii**) no previous diagnosis of GBM recurrence; (**iv**) no additional anti-GBM treatment but the standard of care (i.e. no antiangiogenic therapy etc.); (**v**) two post-standard-therapeutic follow-up MRI scans without signs for radiological recurrence were performed in a period of maximal one year prior to radiological recurrence; and (**vi**) recurrence was determined by at least two board-certified radiologists in consensus based on the updated Response Assessment in Neuro-Oncology (RANO) criteria (16,17) with clear radiological features of recurrence. Radiological recurrence was defined as endpoint of the study period for each patient.

MRI Data Acquisition

Follow-up MRI examinations were performed every 3 – 6 months or on an unscheduled basis in case of clinical signs of tumor recurrence. MRI data acquisition was carried out on a 3 Tesla whole-body scanner (Trio, Siemens, Erlangen, Germany) equipped with the standard 12-channel head coil. The conventional MRI (cMRI) protocol for diagnosis of brain tumors in clinical routine included, among others, the following sequences: (**i**) an axial fluid-attenuated inversion-

recovery (FLAIR) sequence; (**ii**) an axial diffusion-weighted imaging (DWI) sequence; (**iii**) pre- and post-contrast enhanced (CE) high-resolution three-dimensional (3D) T1-weighted magnetization-prepared rapid acquisition with gradient echo (MPRAGE) sequences; and (**iv**) a gradient echo (GE) dynamic susceptibility contrast (DSC) perfusion MRI sequence with 60 dynamic measurements during administration of 0.1 mmol/kg-bodyweight gadoterate-meglumine (Dotarem, Guerbet) at a rate of 4 ml/s using a MR-compatible injector (Spectris, Medrad). A 20-ml-bolus of saline was injected subsequently at the same rate. The parameters of the cMRI sequences are summarized in **Supplementary Table S1**.

For MR-based examination of microvascular architecture and neovascularization activity using the vascular architecture mapping (VAM) approach, we used a DSC perfusion MRI sequence obtained with a SE echo-planar imaging read out (SE-DSC) using the same parameters and contrast agent injection protocol as described for the routine GE-DSC perfusion MRI (**Suppl. Tab. 1**). Our strategies to minimize patient motion and differences in time to first-pass peak, which may significantly affect the data evaluation, were described previously (13,14).

For MR-based investigation of tissue oxygen metabolism using the quantitative blood-oxygen-level-depended (qBOLD) approach, we performed the following sequences: (**i**) a multi-echo GE sequence and (**ii**) a multi-echo spin echo (SE) sequence for mapping of the transverse relaxation rates R_2^* (= $1/T_2^*$) and R_2 (= $1/T_2$), respectively. All experimental sequences for VAM and qBOLD used the same geometric parameters (voxel size, number of slices, etc.) and identical slice position as for the routine GE-DSC perfusion sequence (**Suppl. Tab. 1**). The additional acquisition time (TA) for the VAM sequences (SE-DSC perfusion: TA, 2 min) and qBOLD (R_2^* and R_2-mapping: TA, 1.5 and 3.5 min) was seven minutes.

MRI Data Processing and Retrospective Quantitative Analysis

Processing of cMRI, VAM, and qBOLD data as well as calculation of MRI biomarkers was performed with custom-made MatLab (MathWorks, Natick, MA) software. Details of the MRI data processing pipeline were published previously (11–14) and are described in **Supplementary Figure S1A**. The procedure resulted in the MRI biomarker maps for microstructural density (ADC), macrovascular (CBV) and microvascular perfusion (μCBV), microvascular architecture including microvessel density (MVD) and vessel size index (VSI), neovascularization activity represented by the microvessel type indicator (MTI), and oxygen metabolism including oxygen extraction fraction (OEF), cerebral metabolic rate of oxygen ($CMRO_2$), and tissue oxygen tension (PO_2). All 9 biomarker maps are summarized at the bottom of **Supplementary Figure S1A**.

A retrospective quantitative analysis of the MRI biomarker data was conducted in order to obtain the time courses of the dynamic changes in the 9 physiological parameters that occurred prior to recurrence of GBM after standard therapy. This was executed in four steps starting firstly with definition of regions of interest (ROIs) on the CE T1-weighted MRI with clear radiological features of GBM recurrence, i.e. the endpoint of the study period for an individual patient. Secondly, these ROIs were transferred to the previous follow-up MRI data without signs of GBM recurrence (first and second follow-up). In a third step, MRI biomarker maps were coregistered to the respective CE T1w MRIs, the ROIs were copied, and the mean MRI biomarker values were computed. Finally, the MRI biomarker values were plotted against the time difference between the date of the follow-up MRI and the date of radiological recurrence, i.e. the time before recurrence (TBR; in days), which resulted in the time courses of the MRI biomarkers. Details of the procedure are described in **Supplementary Figure S1B**.

Local GBM recurrence was defined as tumor progression within the wall of the resection cavity or within 20 mm from the margin, and distant GBM recurrence at more than 20 mm from the margin of the resection cavity (18).

Statistical Analysis

Statistical analyses were performed using R (version 3.6.3, R Foundation) and SPSS (version 21, IBM, Chicago, IL, USA). For the scatter plots of MRI biomarker values versus TBR nonparametric regressions were performed using locally estimated scatterplot smoothing (LOESS) functions in order to obtain smooth curves. The LOESS trend lines were graphically analyzed for dynamic physiological changes that precede GBM recurrence. A two-sample Kolmogorov-Smirnov test was used to search for significant differences in the biomarker distribution between local and distant recurrences. Furthermore, the MRI biomarker values were quarterly pooled for further statistical analysis. Significance of differences in quarterly pooled MRI biomarker values between locally and distantly recurrent GBM was calculated using a Mann-Whitney *U* test. Significance of differences in MRI biomarkers between the four quarters to recurrence and to radiological GBM recurrence within the two subgroups (local and distant recurrence) was determined using the one-way analysis of variance (ANOVA) method. The Tukey test was used as post-hoc procedure to be consistent with the assumption that homogeneity of variance was met and for correction for multiple comparisons. Homogeneity of variance was verified using the Levene's test. When the assumption of homogeneity of variances was violated, Welch's ANOVA in combination with the Games-Howell post-hoc test was used. *P* values less than 0.05 were considered to indicate significance.

Results

Patient Characteristics

The institutional database contained almost 1200 MR examinations using the study MRI protocol in 400 patients with brain tumors. From these, 106 patients suffered from brain tumors other than glioma (e.g. brain metastasis or cerebral lymphoma) and 103 patients had a low-grade (WHO grade II) or anaplastic glioma (WHO grade III), respectively. Furthermore, 135 GBM patients were excluded because these patients had none or only one post-standard-therapeutic follow-up MRI scans without signs for radiological recurrence.

This resulted in a total of 56 patients (37 males; 60.8 ± 11.5 years; 29 – 80 years) who fulfilled the study inclusion criteria. Forty-nine patients (87.5%) showed a local recurrence of the GBM, and from these, 11 patients (19.6%) developed a distant recurrence too, i.e. a combined tumor recurrence pattern. Seven patients (12.5%) only had a distantly recurrent GBM. Thus, in total 18 patients suffered from a distant recurrence of the tumor. The mean time between first diagnosis and recurrence was 14.5 ± 6.6 months (5.6 – 31 months). Five patients (8.9%) initially had a glioblastoma with a mutation of the IDH1 gene. A gross-total resection of the initial GBM was achieved in 26 patients (46.5%), a near-total resection in 25 patients (44.6%), and a subtotal resection in 5 patients (8.9%). Treatment of the recurrent GBM included a repeat craniotomy in 27 patients (48.2%, pathology confirmed GBM recurrence in all cases), a temozolomide rechallenge in 12 patients (21.5%), repeat radiation therapy or repeat combined radiochemotherapy in 6 patients (10.7%), second-line monotherapy with the antiangiogenic drug bevacizumab in 6 patients (10.7%), and palliative care without further treatment of the tumor in 5 patients (8.9%). **Supplementary Figures S2** shows an example for a repeat craniotomy of a recurrent GBM.

Dynamic Changes in Physiological Follow-up MRIs of Individual Patients

Calculation of MRI biomarker maps for perfusion (CBV, μCBV), microvascular architecture (MVD, VSI), neovascularization activity (MTI), and oxygen metabolism (OEF, $CMRO_2$, PO_2) was successfully performed for all 168 MRI examinations of all 56 patients. These MRI biomarker maps but not cMRI provided indications for early changes in tissue physiology which occurred prior to recurrence of GBM in humans. **Figure 1** shows an illustrative case depicting two follow-up MRI examinations (**Fig. 1A** and **B**) without signs for recurrence in cMRI (CE T1w, FLAIR, and CBV) but changes (red arrows) in microvascular perfusion (μCBV) and microvascular architecture (MVD) as well as increasing hypoxia (decreasing PO_2) and neovascularization activity (MTI) in the second follow-up (95 days prior to radiological recurrence; **Fig. 1B**). At radiological recurrence (**Fig. 1C**), massive contrast enhancement and peritumoral edema were recognized accompanied by increased perfusion (CBV and μCBV), microvascular architecture (MVD), and neovascularization activity (MTI) as well as a recovery of the tissue oxygen tension (increased PO_2) to normal levels (and even higher).

The most interesting aspect of another representative case (**Fig. 2**) was the very regional hypoxia (low PO_2) that was detected 176 day before radiological recurrence (enlarged image section in the rightmost image of **Fig. 2B**). This small hypoxic region might have been the starting point that initiated upregulation of neovascularization activity leading to increased perfusion and microvascular architecture as well as recovery of the tissue oxygen tension, massive contrast enhancement and peritumoral edema at radiological recurrence almost half a year later (**Fig. 2C**). A further representative case with distant GBM recurrence and less pronounced pathophysiological changes is presented in **Supplementary Figure S3**.

Time Courses of MRI biomarker changes preceding radiological GBM recurrence

The MRI biomarker values obtained from 147 MRI examinations of the 49 patients who developed local recurrence of the GBM were plotted against the time before radiological recurrence (TBR in days) of the tumor. The same procedure was carried out separately with the MRI biomarker data from 54 MRI examinations in 18 patients with distant recurrence of the GBM. The resulting time courses provided information about the dynamic changes in perfusion, microstructural density, microvascular architecture, neovascularization activity, and oxygen metabolism that occurred before and during the development of local and distant recurrence of GBM, respectively (**Fig. 3**).

Both macrovascular (CBV) and microvascular perfusion (μCBV) revealed similar time courses for both local and distant GBM recurrence (**Figs. 3A** and **B**). The values for CBV and μCBV showed a constant course until they increased from 120 days to radiological recurrence. It's noteworthy that the increase was a little stronger for μCBV, i.e. microvascular perfusion (**Fig. 3B**) increased faster compared to macrovascular perfusion (**Fig. 3A**). The density of microvessels (MVD), however, revealed a continuous decrease during the first two quarters that was intensified at about 190 days and reached a clear minimum at about 120 days prior to radiological recurrence. This was followed by a strong increase in MVD (**Fig. 3D**). VSI, the second parameter for microvascular architecture (**Fig. 3E**), however, showed a fairly opposite course in the one-year period to recurrence which was in accordance with previous findings (11): Microvasculature either shows high density of vessels with small lumen or low density of large-lumen vessels. Notwithstanding, 40 days before radiological recurrence a divergence from this principal tendency was observed, namely a simultaneous increase of both the mean vessel density and diameter. In other words, these findings indicated that early neovascularization activity (120 – 40 days to radiological recurrence) was more dominated by formation of smaller vessels which were transformed into larger-lumen vessels during later phases of tumor

vasculature development. Compared to that, the time course of MTI was found to be rather simple and demonstrated an upregulation of neovascularization activity at about 120 days prior to radiological GBM recurrence (**Fig. 3F**).

The time courses of the MRI biomarkers for oxygen metabolism revealed marked differences between local and distant recurrence. For tissue that developed in the further course into local recurrence of a GBM, OEF (**Fig. 3G**,) showed an inverse course compared with microvessel density (MVD) over the whole one-year period: a rather strong increase over the first two quarters which was even intensified at about 190 days and reached its maximum at 120 days prior to radiological recurrence. This was followed by a strong decrease due to the development of a tumor vasculature enabling adequate blood supply and eventually hyperperfusion. The metabolic rate of oxygen ($CMRO_2$, data in cyan in **Fig. 3H**), however, was rather constant over the first two quarters, started to increase at about 190 days to recurrence, and reached the maximum at about 60 days, which was 60 days later than the extrema of the other parameters. This means that $CMRO_2$ showed a time lag in the course compared to OEF and MVD. Consequently, tissue oxygen tension (PO_2, data in cyan in **Fig. 3I**), which is influenced by both OEF and $CMRO_2$, showed a decrease (i.e. increasing hypoxia) from the second quarter that was even intensified at a TBR of about 190 days and reached its minimum value (i.e. maximum hypoxia) at 90 days prior to radiological recurrence.

This clearly demonstrated a close correlation between the dynamics of perfusion (especially µCBV), microvessel architecture (especially MVD) and oxygen metabolism in the one-year period prior to local recurrence. The time of the OEF maximum and the MVD and µCBV minima was coincidently at 120 days. Remarkably, however, the maximum for $CMRO_2$ (TBR of 60 days) and consequently the minimum for PO_2 (TBR of 90 days) occurred closer to the time of radiological recurrence, which was indicative of a metabolic switch from oxidative phosphorylation to aerobic glycolysis, also known as the Warburg effect, which is associated

with a switch from an infiltrative to a proliferative phenotype (19). The time courses of the ADC values (**Fig. 3C**, data in cyan) were supportive for this explanation, because these reveal a decrease of microstructural density (increasing ADC values) until 120 days prior to recurrence followed by an increase in microstructural density (decreasing ADC) probably due to tumor cell proliferation. The decrease in microstructural density in tissue that developed in the further course into local GBM recurrence, however, might be associated with post-radiotherapeutic effects (20). It is noteworthy that oxygen metabolism in brain tissue that developed in the further course into distant GBM recurrence (data in red in **Figs. 3G – I**) was rather constant over the first two quarters and the changes were weaker and occurred later compared to those for local recurrences. This might be explained by additional local effects of radiotherapy which was previously associated with post-therapeutic tissue hypoxia (21).

Model for the physiological changes preceding GBM recurrence

Models for the physiological changes that occur during development of local and distant GBM recurrence (**Figs. 4A** and **B**), respectively, were obtained via combination of the comprehensive data from the different time courses (**Fig. 3**). The diagrams provide insight into the interdependencies between vessel density/perfusion (as a combined parameter), tissue oxygen tension (i.e. hypoxia), neovascularization activity, and microstructural density which preceded radiological recurrence of GBM in humans. The scenario might be as follows:

During the first half of the one-year period to local GBM recurrence, post-radiotherapeutic effects cause a continuous decrease in local vessel density/perfusion, oxygen tension, and microstructural density. Approximately 190 days prior to radiological recurrence incipient cooption of GBM cells to microvessels induces vessel regression which is associated with an additional decrease in vessel density/perfusion and oxygen tension (i.e. intensified hypoxia; **Fig. 4A**). After about 70 days of intensified decrease (at TBR of 120 days), the minimum of vessel

density/perfusion is reached at 50% of the initial level because neovascularization activity is upregulated and starts to promote a strong continuous increase of vessel density/perfusion until recurrence of the GBM is radiologically detected. Additionally at TBR of 120 days, microstructural density also begins to increase slowly but continuously due to tumor cell proliferation. Tissue oxygen tension, however, continues to decrease over a further 30 days after initiation of neovascularization and reaches its minimum 90 days prior to radiological recurrence. At radiological detection of GBM recurrence, vessel density/perfusion reaches on average 170% and tissue oxygen tension 125% of the initial level at the beginning of the one-year period. The model for the distantly recurrent GBM is very similar. The crucial turning points, however, occur 10 days later, possibly due to statistical fluctuations, and the minima were higher (**Fig. 4B**).

Differences between local and distant recurrence

Statistical analysis of the quarterly pooled MRI biomarker data revealed that the most significant differences between the development of local and distant GBM recurrences (marked by a "†" in **Supplementary Figure S4**), respectively, existed for MVD (for 2^{nd} and 3^{rd} quarter) and oxygen metabolism: OEF and $CMRO_2$ for the 3^{rd} and 4^{th} quarter and PO_2 for the 3^{rd} and 4^{th} quarter as well as at radiological recurrence. In other words, the dynamics of changes in microvascular density and oxygen metabolism (including hypoxia) were significantly stronger for local recurrence compared to distant recurrence.

On the other hand, locally recurrent GBM per se showed more significant differences between the quarters (marked by a "*" in **Supplementary Figure S4**) compared to distantly recurrent GBM. During local GBM recurrence, CBV, μCBV, MVD, and $CMRO_2$ increased significantly from the 3^{rd} to the 4^{th} quarter and from the 4^{th} quarter to radiological recurrence. Only oxygen metabolism, however, revealed significant early changes half a year prior to local radiological

recurrence: OEF and $CMRO_2$ increased significantly and PO_2 decreased (i.e. tissue hypoxia increased) significantly from the 2nd to the 3rd quarter (**Supplementary Figure S4**).

Discussion

Recurrence is an inevitable event in the course of disease of most GBM patients and poses a major diagnostic and therapeutic challenge as recurrent GBMs are commonly detected at an advanced stage, which limits the choice of treatment options. Gross-total resection of GBM recurrence is associated with significantly longer overall survival compared with no surgery or subtotal resection (22) and should, therefore, be performed whenever possible in patients with recurrent GBM. However, early and reliable detection of GBM recurrence is essential to enable the most radical repeat resection of the tumor.

In this study, we applied an extended MRI protocol, which is fully compatible with the requirements of clinical routine diagnostics (11,13), to search for early alterations in macro- and microvascular perfusion, microvascular architecture, neovascularization activity, oxygen metabolism (including tissue hypoxia), and microstructural density that occurred during development of recurrence in GBM patients. These physiological MRI biomarkers were introduced and used in previous studies. The novelty of the present study, however, is the non-invasive investigation of the dynamic pathophysiological changes that precede the recurrence of GBM over a period of one year using these biomarkers. Our main findings were threefold: (**i**) Our MRI approach enabled detection of early pathophysiological changes during development of GBM recurrence; (**ii**) We developed a model describing the dynamic changes and the interdependence of the physiological parameters that precede GBM recurrence; and (**iii**) Differences in the pathophysiological development of locally and distantly recurrent GBM were dominated by post-radiotherapeutic effects.

The earliest pathophysiological alteration, that was detected with our MRI approach and might be associated with the development of GBM recurrence, occurred 190 days prior to radiological detection of recurrence. We observed a decrease in microvascular density with accompanied increases in oxygen extraction from vasculature and tissue hypoxia. This might be related to vascular cooption of GBM cell and formation of cuffs around microvessel (7). It is well-known that coopted vessels express ANG-2, which in absence of VEGF promotes endothelial cell apoptosis and vessel regression (9), that could have been macroscopically detected as decreasing MVD with our MRI approach. Zagzag et al. (23) identified in a temporal study on a murine glioma model vascular co-option as an initial step of a cascade of events. By using transmission electron microscopy (TEM), they observed vascular co-option 1 week after glioma cell (GL261) implantation followed by endothelial cell apoptosis and vascular regression after 3 weeks. Involution of coopted vessels resulted in tumor hypoxia, upregulation of proangiogenic factors (hypoxia-induced VEGF expression), and a shift toward an angiogenic phenotype after 4 weeks. In our study the effects of the angiogenic switch (increasing MVD, CBV, μCBV, and MTI) were macroscopically observed 70 days after the assumed onset of vascular cooption and 120 day prior to detection of recurrence in cMRI. The significant difference in the time to the angiogenic switch (3 weeks vs. 10 weeks) may be caused by the different study designs: microscopic investigation with TEM of implanted glioma cells in mouse brains vs. macroscopic investigation with MRI of recurrent GBM in patients. Furthermore, this could also be heavily influenced by differences in treatment which patients vs. these mice received.

A continuous increase in tissue hypoxia (decrease in PO_2) preceding the angiogenic switch was observed in our study too. Interestingly, hypoxia continued to increase over another 30 days after the angiogenic switch, which might be required to maintain and intensify the neovascularization activity. Otherwise, i.e. without continued hypoxia after the angiogenic switch, the neovascular progression might be totally or in part be suppressed. This was a very

interesting and unexpected finding of our study, since it could open up the possibility of developing new combined monitoring-treatment options tailored for recurrent GBM. Taking these study observations into account, a potential strategy could be as follows: Follow-up examinations including our physiological MRI approach are used to search for increasing MVD and μCBV, MTI values suspect for incipient neovascularization activity combined with decreasing PO_2 (increasing hypoxia). If this pattern is detected one could initiate antiangiogenic (24) or antihypoxic therapy (25,26) or a combined treatment targeting both angiogenesis and hypoxia (27). Of course, repeat gross-total resection or minimal-invasively stereotactic laser ablation (28) recurrent GBM may be an alternative treatment options too.

The usefulness of cMRI and PET for GBM recurrence prediction was already investigated in previously published in-human studies. Chang et al. (29) studied postoperative cMRIs of 26 of patients with native GBM immediately after undergoing gross total tumor resection and before chemoradiotherapy. Retrospective voxel-wise histogram analysis revealed that voxels of future GBM recurrence within the peritumoral region showed small but statistically significant signal loss on ADC and anatomic FLAIR images months before the development of abnormal enhancement occurs. Furthermore, they calculated probability maps of tumor recurrence based on multiparametric logistic regression model using these signal changes. Metz et al. (30) even evaluated preoperative maps of fractional anisotropy and found significant differences between the areas of recurrence-free edema and areas with later GBM recurrence. However, the usefulness of these approaches for follow-up monitoring after chemoradiotherapy remains largely unknown. Furthermore, a prospective follow-up study after standard therapy concluded that conventional perfusion (macrovascular CBV) and diffusion MRI (ADC) do not reliably predict the GBM relapse sites (31), which is in line with our results. Two further studies (32,33) compared postoperative cMRI and ^{18}F-fluoroethyl-tyrosine (FET) PET data for prediction of GBM recurrence and revealed the superiority of metabolic imaging for that purpose. We chose a

similar but MRI-based approach in our study by consideration of oxygen metabolism, neovascularization activity, and microvascular architecture for early GBM recurrence detection.

There are several limitations in our study. Our VAM approach was limited by the requirement for an additional DSC MRI perfusion sequences (SE-DSC) and a separate contrast agent injection. However, this ensures that the GE-DSC perfusion sequence, which is essential for clinical routine diagnosis, was kept unchanged regarding spatial and temporal resolution. Therefore, our approach allows the acquisition of VAM data with high signal-to-noise ratio, high spatial resolution, and coverage of the whole brain, which is mandatory for in clinical routine. These features are especially important for detection of small or multi-centric lesions. The commonly used combined simultaneous GE-SE-DSC perfusion sequences (34–36), however, does not meet these requirements and necessitate performing the routine perfusion separately requiring an additional contrast agent injection. Furthermore, the combined simultaneous GE-SE-DSC perfusion sequence was performed with a double dose or more (34–36). This resulted in the application of up to a triple-dose. The model for assessment of oxygen metabolism has also several limitations. It assumes that the system is in the static dephasing regime (37) which is associated with the fact that OEF is predominantly weighted to the medium sized and larger vessels of the venous vascular network. Furthermore, the multiparametric qBOLD approach (38) provides an average blood oxygenation within the entire vasculature, which is different from the venous blood oxygenation (deoxygenated CBV) derived from the original qBOLD approach (39), and ignores the intravascular component. Additionally, accumulation of hemosiderin and/or proteins as well as non-BOLD susceptibility effects (R2*; due to uncorrectable macroscopic background gradients or white matter fiber orientation) and contrast agent leakage could bias the OEF estimation (40–42). Therefore, it is important to point out that the multiparametric qBOLD approach provides only an estimation of the oxygen metabolism with model-inherent limitations. The number of patients with local (N = 49) and especially distant recurrence (N = 18)

was relatively small which was related to our rather strict inclusion criteria. We performed a retrospective analysis of our prospectively obtained physiological MRI data. Prospective studies evaluating the clinical usefulness of our pathophysiological model of GBM recurrence deserve further attention. It is also important to note that a clear distinction between therapy-related changes in oxygen metabolism and microvascular architecture was not possible with our imaging approach. The causes of the physiological changes prior to GBM recurrence, as described in the present study, as well as the models that were developed are hence speculative. Therefore, histological and biological validation of our findings is required by correlation with results from immunohistochemistry or invasive methods using animal models as well as from clinical PET data of the same patients.

Conclusions

Conclusively, we were able to describe time courses of the pathophysiological tumor characteristics that occur prior to the recurrence of GBM in patients after standard therapy. These findings might be helpful to implement both new MR-based imaging modalities for routine follow-up monitoring of GBM patients after standard therapy and novel therapy options which, if combined, could enable earlier and specially tailored treatment of recurrent GBM. However, further preclinical as well as prospective in-human studies are required for validation, evaluation and application of our findings.

Acknowledgment. This work was supported by the German Research Foundation (Deutsche Forschungsgemeinschaft – DFG; Grant Numbers STA 1331/3-1; A. Stadlbauer).

References

1. Lemee JM, Clavreul A, Menei P. Intratumoral heterogeneity in glioblastoma: Don't forget the peritumoral brain zone. Neuro Oncol. 2015;17:1322–32.

2. Hou LC, Veeravagu A, Hsu AR, Tse VCK. Recurrent glioblastoma multiforme: a review of natural history and management options. Neurosurg Focus. 2006;20:E5.

3. Campos B, Olsen LR, Urup T, Poulsen HS. A comprehensive profile of recurrent glioblastoma. Oncogene. 2016;35:5819–25.

4. Seano G, Jain RK. Vessel co-option in glioblastoma: emerging insights and opportunities. Angiogenesis. 2020;23:9–16.

5. Montana V, Sontheimer H. Bradykinin promotes the Chemotactic invasion of primary brain tumors. J Neurosci. 2011;31:4858–4867.

6. Griveau A, Seano G, Shelton SJ, Kupp R, Jahangiri A, Obernier K, et al. A Glial Signature and Wnt7 Signaling Regulate Glioma-Vascular Interactions and Tumor Microenvironment. Cancer Cell. 2018;33:874–89.

7. Hardee ME, Zagzag D. Mechanisms of glioma-associated neovascularization. Am J Pathol. 2012;181:1126–41.

8. Watkins S, Robel S, Kimbrough IF, Robert SM, Ellis-Davies G, Sontheimer H. Disruption of astrocyte-vascular coupling and the blood-brain barrier by invading glioma cells. Nat Commun. 2014;5:4196.

9. Holash J, Maisonpierre PC, Compton D, Boland P, Alexander CR, Zagzag D, et al. Vessel cooption, regression, and growth in tumors mediated by angiopoietins and VEGF. Science. 1999;284:1994–8.

10. Hambardzumyan D, Bergers G. Glioblastoma: Defining Tumor Niches. Trends in cancer. 2015;1:252–65.

11. Stadlbauer A, Zimmermann M, Heinz G, Oberndorfer S, Doerfler A, Buchfelder M, et al. Magnetic resonance imaging biomarkers for clinical routine assessment of microvascular architecture in glioma. J Cereb blood flow Metab. 2017;37:632–43.

12. Stadlbauer A, Zimmermann M, Doerfler A, Oberndorfer S, Buchfelder M, Coras R, et al. Intratumoral heterogeneity of oxygen metabolism and neovascularization uncovers 2 survival-relevant subgroups of IDH1 wild-type glioblastoma. Neuro Oncol. 2018;20:1536–46.

13. Stadlbauer A, Zimmermann M, Kitzwögerer M, Oberndorfer S, Rössler K, Dörfler A, et al. MR Imaging–derived Oxygen Metabolism and Neovascularization Characterization for Grading and IDH Gene Mutation Detection of Gliomas. Radiology. 2017;283:799–809.

14. Stadlbauer A, Mouridsen K, Doerfler A, Bo Hansen M, Oberndorfer S, Zimmermann M, et al. Recurrence of glioblastoma is associated with elevated microvascular transit time heterogeneity and increased hypoxia. J Cereb blood flow Metab. 2018;38:422–32.

15. Stupp R, Mason WP, van den Bent MJ, Weller M, Fisher B, Taphoorn MJB, et al. Radiotherapy plus concomitant and adjuvant temozolomide for glioblastoma. N Engl J Med. 2005;352:987–96.

16. Wen PY, Macdonald DR, Reardon DA, Cloughesy TF, Sorensen AG, Galanis E, et al. Updated response assessment criteria for high-grade gliomas: Response assessment in neuro-oncology working group. J Clin Oncol. 2010;28:1963–72.

17. Ellingson BM, Wen PY, Cloughesy TF. Modified Criteria for Radiographic Response Assessment in Glioblastoma Clinical Trials. Neurotherapeutics. 2017;14:307–20.

18. Konishi Y, Muragaki Y, Iseki H, Mitsuhashi N, Okada Y. Patterns of intracranial glioblastoma recurrence after aggressive surgical resection and adjuvant management: retrospective analysis of 43 cases. Neurol Med Chir (Tokyo). 2012;52:577–86.

19. Xie Q, Mittal S, Berens ME. Targeting adaptive glioblastoma: an overview of proliferation and invasion. Neuro Oncol. 2014;16:1575–84.

20. Hein PA, Eskey CJ, Dunn JF, Hug EB. Diffusion-Weighted Imaging in the Follow-up of Treated High-Grade Gliomas: Tumor Recurrence versus Radiation Injury. Am J Neuroradiol. 2004;25:201–9.

21. Gupta K, Burns TC. Radiation-induced alterations in the recurrent glioblastoma microenvironment: Therapeutic implications. Front Oncol. 2018;8:Article 503.

22. Lu VM, Jue TR, McDonald KL, Rovin RA. The Survival Effect of Repeat Surgery at Glioblastoma Recurrence and its Trend: A Systematic Review and Meta-Analysis. World Neurosurg. 2018;115:453–9.

23. Zagzag D, Amirnovin R, Greco MA, Yee H, Holash J, Wiegand SJ, et al. Vascular apoptosis and involution in gliomas precede neovascularization: a novel concept for glioma growth and angiogenesis. Lab Invest. 2000;80:837–49.

24. Potente M, Gerhardt H, Carmeliet P. Basic and therapeutic aspects of angiogenesis. Cell. 2011;146:873–87.

25. Paolicchi E, Gemignani F, Krstic-Demonacos M, Dedhar S, Mutti L, Landi S. Targeting hypoxic response for cancer therapy. Oncotarget. 2016;7:13464–78.

26. Wilson WR, Hay MP. Targeting hypoxia in cancer therapy. Nat Rev Cancer. 2011;11:393–410.

27. Jain RK. Antiangiogenesis Strategies Revisited: From Starving Tumors to Alleviating Hypoxia. Cancer Cell. 2014;26:605–22.

28. Hawasli AH, Kim AH, Dunn GP, Tran DD, Leuthardt EC. Stereotactic laser ablation of high-grade gliomas. Neurosurg Focus. 2014;37:E1.

29. Chang PD, Chow DS, Yang PH, Filippi CG, Lignelli A. Predicting Glioblastoma Recurrence by Early Changes in the Apparent Diffusion Coefficient Value and Signal Intensity on FLAIR Images. Am J Roentgenol. 2017;208:57–65.

30. Metz M-C, Molina-Romero M, Lipkova J, Gempt J, Liesche-Starnecker F, Eichinger P, et al. Predicting Glioblastoma Recurrence from Preoperative MR Scans Using Fractional-Anisotropy Maps with Free-Water Suppression. Cancers (Basel). 2020;12:728.

31. Khalifa J, Tensaouti F, Lotterie J-A, Catalaa I, Chaltiel L, Benouaich-Amiel A, et al. Do perfusion and diffusion MRI predict glioblastoma relapse sites following chemoradiation? J Neurooncol. 2016;130:181–92.

32. Buchmann N, Gempt J, Ryang Y-M, Pyka T, Kirschke JS, Meyer B, et al. Can Early Postoperative O-(2-18FFluoroethyl)-l-Tyrosine Positron Emission Tomography After Resection of Glioblastoma Predict the Location of Later Tumor Recurrence? World Neurosurg. 2019;121:e467–74.

33. Lundemann M, Munck af Rosenschöld P, Muhic A, Larsen VA, Poulsen HS, Engelholm S-A, et al. Feasibility of multi-parametric PET and MRI for prediction of tumour recurrence in patients with glioblastoma. Eur J Nucl Med Mol Imaging. 2019;46:603–13.

34. Sorensen AG, Batchelor TT, Zhang W-T, Chen P-J, Yeo P, Wang M, et al. A “Vascular Normalization Index” as Potential Mechanistic Biomarker to Predict Survival after a Single Dose of Cediranib in Recurrent Glioblastoma Patients. Cancer Res. 2009;69:5296–300.

35. Eichner C, Jafari-Khouzani K, Cauley S, Bhat H, Polaskova P, Andronesi OC, et al. Slice accelerated gradient-echo spin-echo dynamic susceptibility contrast imaging with blipped CAIPI for increased slice coverage. Magn Reson Med. 2014;72:770–8.

36. Emblem KE, Mouridsen K, Bjornerud A, Farrar CT, Jennings D, Borra RJ, et al. Vessel architectural imaging identifies cancer patient responders to anti-angiogenic therapy. Nat Med. 2013;19:1178–83.

37. Yablonskiy DA, Haacke EM. Theory of NMR signal behavior in magnetically inhomogeneous tissues: The static dephasing regime. Magn Reson Med. 1994;32:749–63.

38. Christen T, Schmiedeskamp H, Straka M, Bammer R, Zaharchuk G. Measuring brain oxygenation in humans using a multiparametric quantitative blood oxygenation level dependent MRI approach. Magn Reson Med. 2012;68:905–11.

39. He X, Yablonskiy DA. Quantitative BOLD: Mapping of human cerebral deoxygenated blood volume and oxygen extraction fraction: Default state. Magn Reson Med. 2007;57:115–26.

40. Hirsch NM, Toth V, Förschler A, Kooijman H, Zimmer C, Preibisch C. Technical considerations on the validity of blood oxygenation level-dependent-based MR assessment of vascular deoxygenation. NMR Biomed. 2014;27:853–62.

41. Kaczmarz S, Göttler J, Zimmer C, Hyder F, Preibisch C. Characterizing white matter fiber orientation effects on multi-parametric quantitative BOLD assessment of oxygen extraction fraction. J Cereb Blood Flow Metab. 2020;40:760–74.

42. Tóth V, Förschler A, Hirsch NM, Den Hollander J, Kooijman H, Gempt J, et al. MR-based hypoxia measures in human glioma. J Neurooncol. 2013;115:197–207.

Figure Legends

Figure 1. Follow-up MRI examinations of a 69-year-old male patient who developed local recurrence of a glioblastoma. In both the first (**A**) and the second (**B**) follow-up, 217 and 95 days prior to radiological recurrence, respectively, conventional anatomic MRI (cMRI; CE T1w and FLAIR) as well as macrovascular perfusion (CBV from conventional GE-DSC perfusion MRI data) showed no signs for changes in the brain area where recurrence finally occurred (**C**). However, microvascular perfusion (μCBV from experimental SE-DSC perfusion MRI data), microvascular architecture (MVD), neovascularization activity (MTI), and tissue oxygen tension (PO_2) revealed physiological changes in the second follow-up (**B**, 95 days before radiological recurrence; TBR = time before radiological recurrence).

Figure 2. Follow-up MRI examinations of a 54-year-old male patient who developed local recurrence of a glioblastoma. Both the first (**A**) and the second (**B**) follow-up MRI (365 and 176 days prior to radiological recurrence) revealed no changes in conventional MRI (cMRI; CE T1w and FLAIR), microvascular and microvascular perfusion (CBV and μCBV), microvascular architecture (MVD), and neovascularization activity (MTI). Most interestingly, tissue oxygen tension (PO_2) demonstrated a very regional hypoxia in the second follow-up (red-rimmed enlarged image section, rightmost in **B**) which might be the precipitating event for GBM recurrence (**C**; TBR = time before radiological recurrence).

Figure 3. Time courses of the dynamic MRI biomarker changes that occurred prior to a local (cyan) or distant recurrence (red) of a glioblastoma, respectively. Scatter plots and locally-estimated-scatterplot-smoothing (LOESS) trend lines of MRI biomarker for **A**) macrovascular perfusion (CBV), **B**) macrovascular perfusion (μCBV), **C**) microstructural density (ADC), microvascular architecture represented by **D**) microvascular density (MVD) and **E**) diameter (VSI), **F**) neovascularization activity (MTI), and oxygen metabolism (**G**: OEF; **H**: $CMRO_2$, and **I**: PO_2) versus time before radiological recurrence (TBR, in days).

Figure 4. Model for the physiological changes that precede local (**A**) and distant recurrence (**B**) of glioblastoma. The diagrams visualize the dynamic relative changes and the interdependence of the parameters microvascular density and perfusion (red line), neovascularization activity (MTI; purple line), tissue oxygen tension (PO_2; light blue line), and microstructural density (ADC; gray line) that occurred during the development of GBM recurrence. Note: A combined parameter was used for microvascular density (MVD) and perfusion (CBV and μCBV) because these biomarkers were very similar. PO_2 represents tissue hypoxia (the lower the PO_2 value the stronger the hypoxia in the tissue). Starting value (100%) was the biomarker value at the beginning of the study period, i.e. one year before radiological recurrence (TBR = time before radiological recurrence).

Figure 1

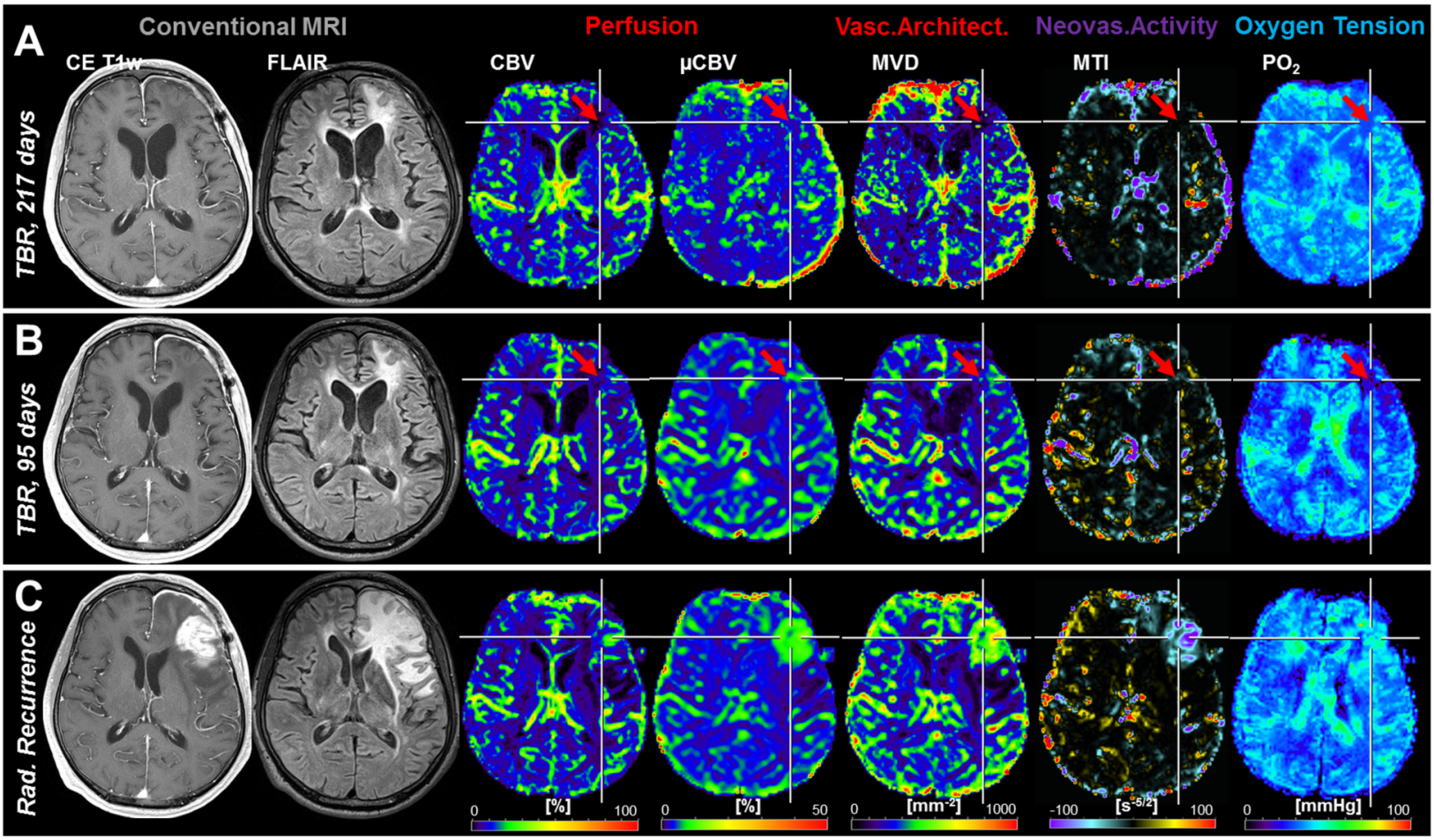

Author Manuscript Published OnlineFirst on December 8, 2020; DOI: 10.1158/1078-0432.CCR-20-3580
Author manuscripts have been peer reviewed and accepted for publication but have not yet been edited.

Figure 2

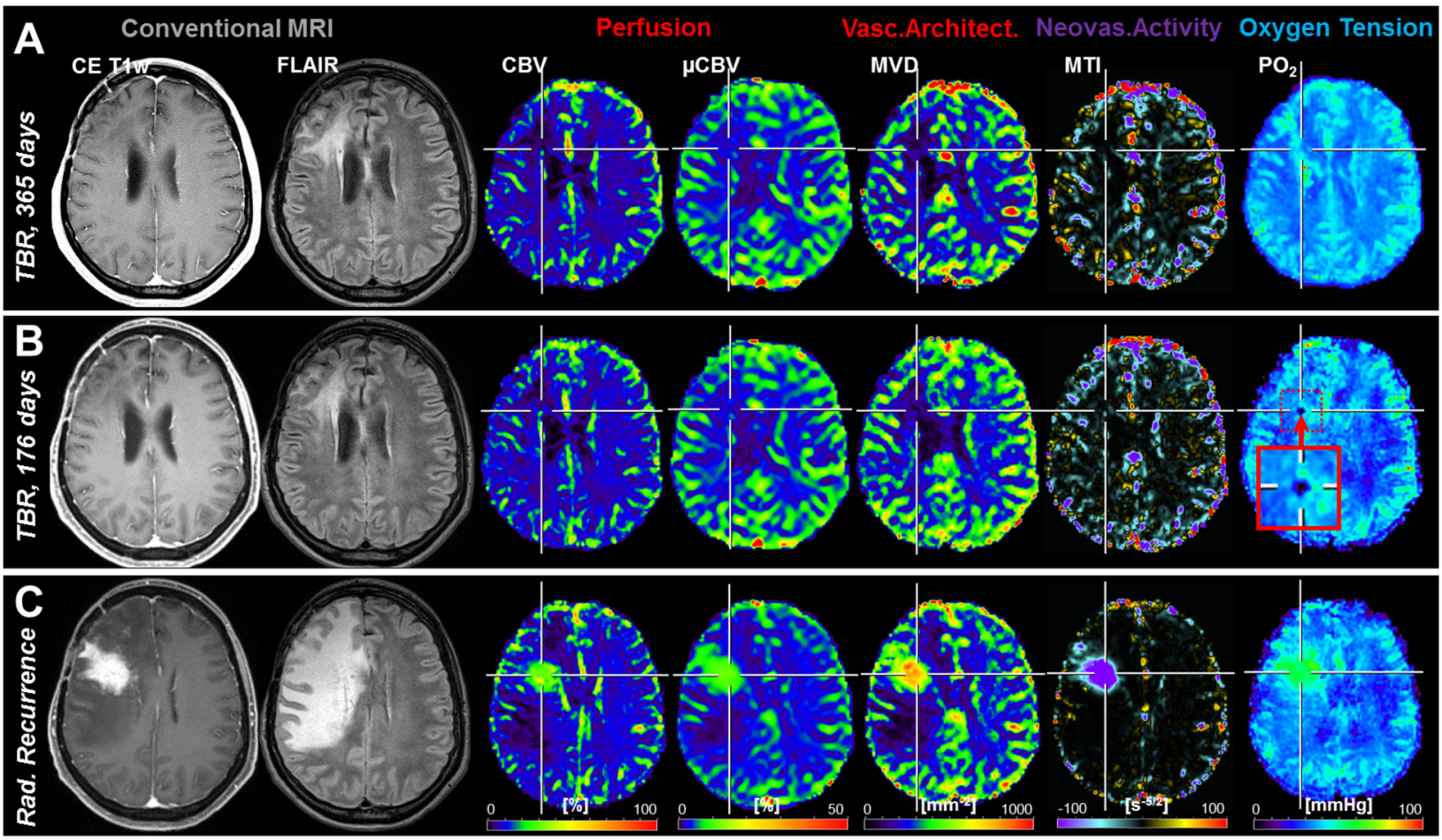

Author Manuscript Published OnlineFirst on December 8, 2020; DOI: 10.1158/1078-0432.CCR-20-3580
Author manuscripts have been peer reviewed and accepted for publication but have not yet been edited.

Figure 3

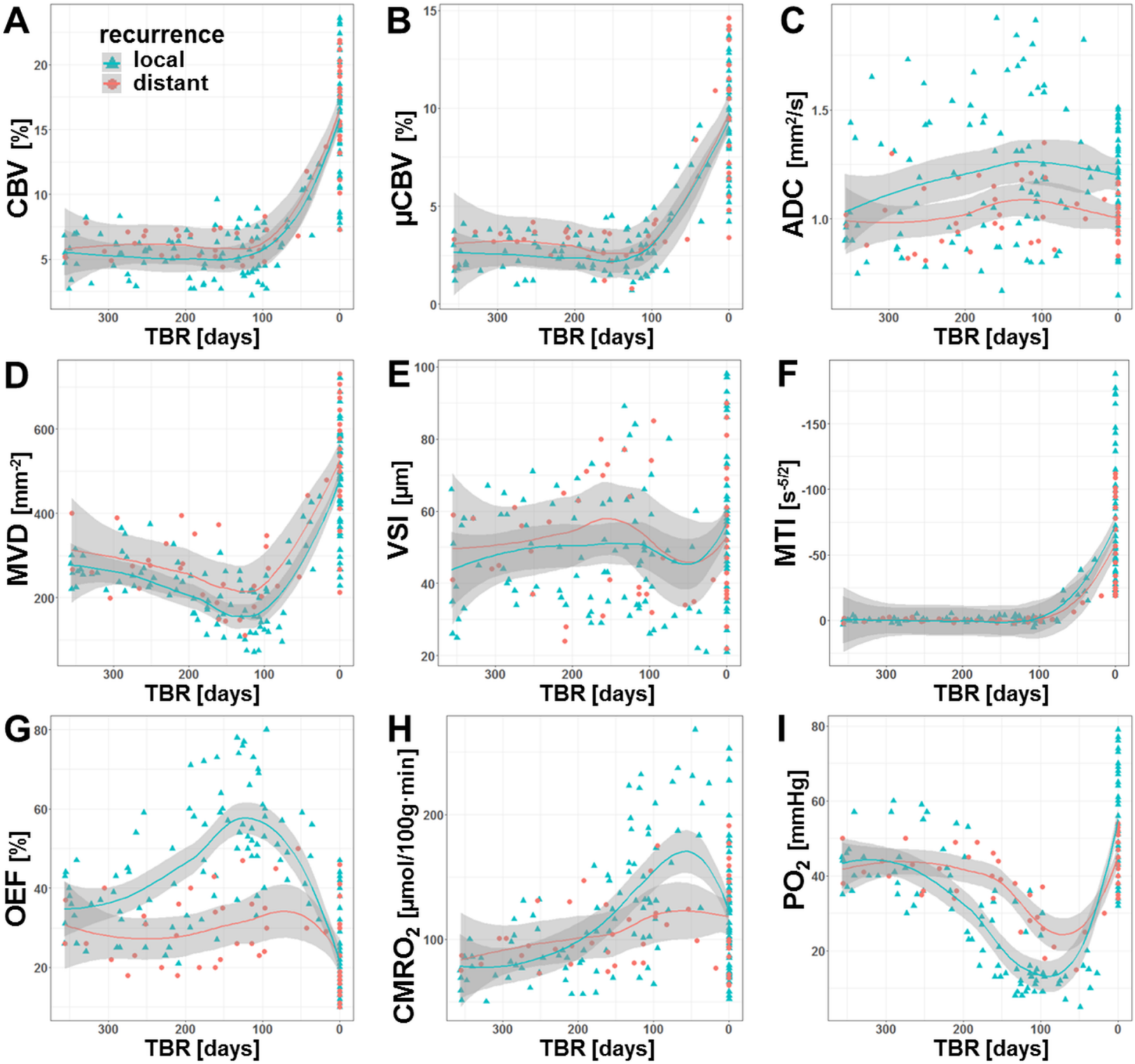

Author Manuscript Published OnlineFirst on December 8, 2020; DOI: 10.1158/1078-0432.CCR-20-3580
Author manuscripts have been peer reviewed and accepted for publication but have not yet been edited.

Figure 4

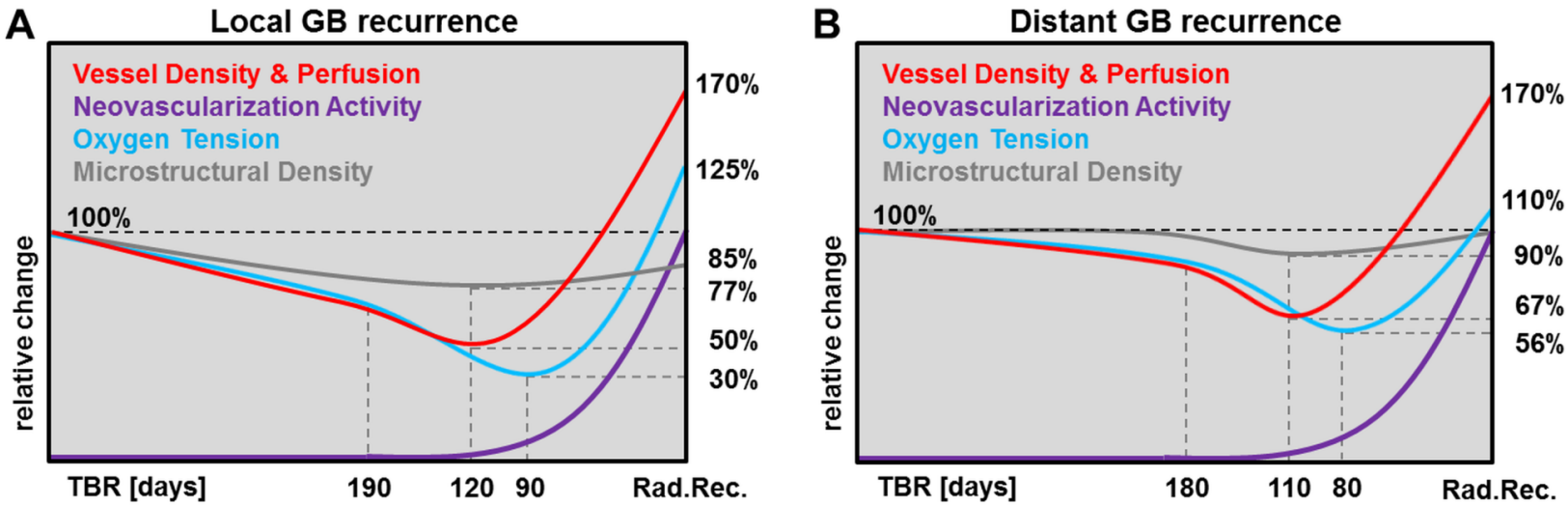

AACR American Association for Cancer Research

Clinical Cancer Research

Tissue hypoxia and alterations in microvascular architecture predict glioblastoma recurrence in humans

Andreas Stadlbauer, Thomas M. Kinfe, Ilker Eyüpoglu, et al.

Clin Cancer Res Published OnlineFirst December 8, 2020.